Activation of ER stress and mTORC1 suppresses hepatic sortilin-1 levels in obese mice

Ding Ai,[1] Juan M. Baez,[1] Hongfeng Jiang,[1] Donna M. Conlon,[1] Antonio Hernandez-Ono,[1] Maria Frank-Kamenetsky,[2] Stuart Milstein,[2] Kevin Fitzgerald,[2] Andrew J. Murphy,[1] Connie W. Woo,[1] Alanna Strong,[3] Henry N. Ginsberg,[1] Ira Tabas,[1] Daniel J. Rader,[3] and Alan R. Tall[1]

[1]Department of Medicine, Columbia University, New York, New York, USA. [2]Alnylam Pharmaceuticals, Cambridge, Massachusetts, USA. [3]Institute for Translational, Medicine and Therapeutics, Institute for Diabetes, Obesity and Metabolism, and Cardiovascular Institute, Perelman School of Medicine at the University of Pennsylvania, Philadelphia, Pennsylvania, USA.

Recent GWAS have identified SNPs at a human chromosom1 locus associated with coronary artery disease risk and LDL cholesterol levels. The SNPs are also associated with altered expression of hepatic sortilin-1 (*SORT1*), which encodes a protein thought to be involved in apoB trafficking and degradation. Here, we investigated the regulation of *Sort1* expression in mouse models of obesity. *Sort1* expression was markedly repressed in both genetic (*ob/ob*) and high-fat diet models of obesity; restoration of hepatic sortilin-1 levels resulted in reduced triglyceride and apoB secretion. Mouse models of obesity also exhibit increased hepatic activity of mammalian target of rapamycin complex 1 (mTORC1) and ER stress, and we found that administration of the mTOR inhibitor rapamycin to *ob/ob* mice reduced ER stress and increased hepatic sortilin-1 levels. Conversely, genetically increased hepatic mTORC1 activity was associated with repressed *Sort1* and increased apoB secretion. Treating WT mice with the ER stressor tunicamycin led to marked repression of hepatic sortilin-1 expression, while administration of the chemical chaperone PBA to *ob/ob* mice led to amelioration of ER stress, increased sortilin-1 expression, and reduced apoB and triglyceride secretion. Moreover, the ER stress target Atf3 acted at the *SORT1* promoter region as a transcriptional repressor, whereas knockdown of *Atf3* mRNA in *ob/ob* mice led to increased hepatic sortilin-1 levels and decreased apoB and triglyceride secretion. Thus, in mouse models of obesity, induction of mTORC1 and ER stress led to repression of hepatic *Sort1* and increased VLDL secretion via Atf3. This pathway may contribute to dyslipidemia in metabolic disease.

Introduction

Increased hepatic VLDL secretion is a characteristic feature of type 2 diabetes and obesity, leading to dyslipidemia characterized by increased triglycerides (TGs) and apoB levels, increased VLDL and LDL cholesterol, reduced HDL, and increased atherosclerosis (1–4). apoB is the major apolipoprotein of VLDL and LDL, which transport TGs and cholesterol from the liver into the bloodstream (5). The regulation of hepatic apoB secretion occurs primarily on a posttranscriptional level and appears to involve intracellular protein degradation both in the ER and post-Golgi (6, 7). The mechanisms underlying the dysregulation of VLDL apoB secretion in obesity are poorly understood.

Recently, human GWAS have identified several novel genetic loci associated with LDL cholesterol levels and coronary artery disease risk. SNPs at a widely replicated chromosome 1p13 locus have been associated with myocardial infarction (MI) and with total and LDL cholesterol levels (8–10). The minor alleles at this locus are present in approximately 20%–35% of individuals of mixed European descent, and homozygosity for the minor alleles, as opposed to homozygosity for the major alleles, is associated with a 20%–40% decrease in the risk of MI and up to 16 mg/dl lower LDL cholesterol levels (10–12). The relevant SNPs are localized in a gene cluster containing 4 genes, *CELSR2*, *PSRC1*, *MYBPHL*, and *SORT1*, and the minor allele is associated with increased *SORT1* expression in the liver. A recent study has provisionally identified the causative SNP at this locus (rs12740374) and shown that it regulates hepatic *SORT1* expression by creating a C/EBPα binding site (11). Sortilin-1 is involved in Golgi to lysosome protein transport (13, 14) and is returned to the Golgi by the retromer complex (15). Sortilin-1 has also been reported to bind and degrade LPL and apoAV (16, 17) and to be involved in the formation and insulin responsiveness of GLUT-4 storage vesicles during adipocyte differentiation (18). In the liver, sortilin-1 may be involved in the post-Golgi regulation of apoB secretion by promoting trafficking of apoB into intracellular, possibly lysosomal, degradation pathways (9). In one report, mouse models with decreased sortilin-1 expression were found to be associated with increased VLDL secretion, whereas increased sortilin-1 expression had the opposite effect (9).

The conserved serine/threonine kinase mammalian target of rapamycin (mTOR) complex 1 (mTORC1) integrates inputs from several upstream pathways, including nutritional stimuli, with the cellular growth machinery (19). mTORC1 triggers increased protein synthesis and ribosomal biogenesis, thereby playing a key role in coupling nutrients to growth (19). mTORC1 has also been implicated in the regulation of hepatic *Srebp1c* and lipogenesis (13, 20–22). The tuberous sclerosis (TSC) tumor suppressor complex,

Conflict of interest: Alan R. Tall serves on scientific advisory boards for Merck and Arisaph Pharmaceuticals and provides paid consulting services to Roche, Merck, Arisaph Pharmaceuticals, and CSL Ltd. related to the development of drugs that would increase HDL levels. Maria Frank-Kamenetsky, Stuart Milstein, and Kevin Fitzgerald serve for Alnylam Pharmaceuticals Inc.

Citation for this article: *J Clin Invest.* 2012;122(5):1677–1687. doi:10.1172/JCI61248.

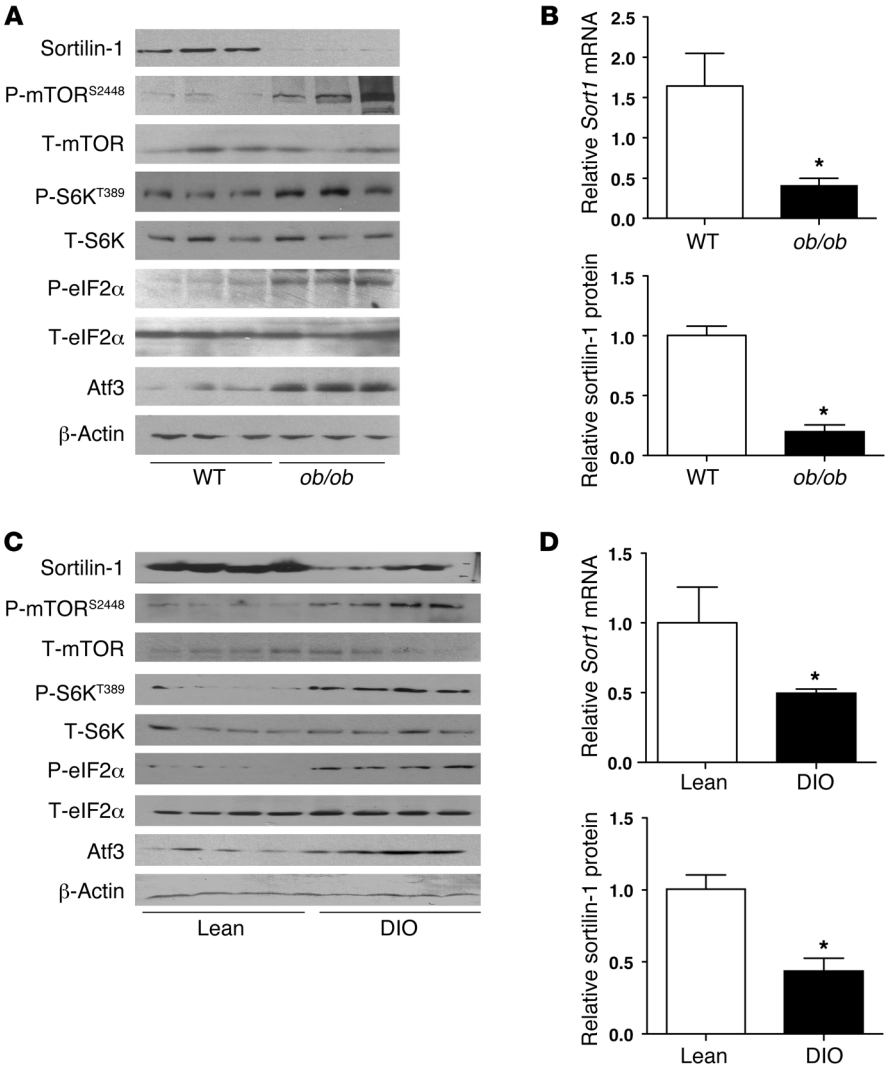

Figure 1
Regulation of sortilin-1 in obesity. Shown are results for (**A** and **B**) *ob/ob* mice (8–10 weeks old) and (**C** and **D**) DIO mice (C57BL/6 fed high-fat diet for 20 weeks). (**A** and **C**) Western blot analysis of hepatic protein levels after a 6-hour fast. β-Actin was used as internal control. P-, phosphorylated; T-, total. (**B** and **D**) Quantification of sortilin-1 protein level and measurement of hepatic *Sort1* mRNA by QPCR. **P* < 0.05, unpaired *t* test.

composed of TSC1 and TSC2, negatively regulates mTORC1 due to increased levels of GTP-bound Rheb (23, 24). Studies in the past decade have shown that genetic and dietary obesity are associated with ER stress (25, 26), secondary to increased mTORC1 activity and increased protein synthesis (27). Hyperinsulinemic, obese *ob/ob* mice show increased hepatic mTORC1 activity (28) and increased hepatic VLDL apoB and TG secretion (29, 30), whereas mice with sustained reductions in insulin signaling as a result of genetic knockdown of insulin receptors show reduced hepatic mTOR activity and decreased VLDL secretion (30). These observations led us to explore a possible link between reduced hepatic *Sort1* expression and obesity, mTORC1, and ER stress, by which this gene potentially mediates increased VLDL secretion in obesity.

Results

Downregulation of hepatic sortilin-1 in mouse models of obesity. To evaluate the regulation of sortilin-1 in obesity, we measured sortilin-1 expression in the livers of both genetic (*ob/ob*) and high-fat diet–induced (0.03% cholesterol, 60% kcal from fat) murine models of obesity. There was a marked decrease in hepatic sortilin-1 protein and mRNA in both models. In *ob/ob* mice and in mice fed high-fat diet for 20 weeks (referred to herein as DIO mice), *Sort1* mRNA levels were reduced by 76% and 50%, and sortilin-1 protein levels by 81% and 57%, respectively (Figure 1, A–D). The livers of *ob/ob* and DIO mice exhibited increased p-mTOR and ER stress markers, such as phosphorylated eIF2α and Atf3 (Figure 1, A and C, and refs. 31, 32). We also examined sortilin-1 expression in the livers of *Ldlr*$^{-/-}$ mice fed for 14 weeks on the Western-type diet (WTD; 0.15% cholesterol, 45% kcal from fat), which is often used in atherosclerosis studies and induces moderate obesity (33). This resulted in repression of sortilin-1 protein and mRNA (40% and 54%, respectively; Supplemental Figure 1, A and B; supplemental material available online with this article; doi:10.1172/JCI61248DS1). A time-course study showed that the repression of sortilin-1 was gradual, with 16% and 44% reductions after 4 and 8 weeks, respectively, of high-fat diet feeding (Supplemental Figure 1C). Repression of sortilin-1 was associated with activation of mTOR and induction of the early-stage ER stress marker Atf3 (Supplemental Figure 1, A and C).

Reconstitution of sortilin-1 in mouse models of obesity leads to reduced VLDL secretion. We have previously shown that hepatic VLDL TG and apoB secretion are increased in *ob/ob* mice (30). To determine whether the reduced expression of sortilin-1 in the livers of *ob/ob* mice was involved in this effect, we reconstituted sortilin-1 expression in *ob/ob* liver using *Sort1*-expressing adeno-associated virus–8 (AAV8-*Sort1*; Figure 2A), followed by injection of the detergent poloxamer 407 (P407) to assess VLDL secretion. Preliminary dose-response titrations of virus were carried out, so as to achieve only moderate expression of hepatic sortilin-1 protein levels in *ob/ob* mice. At 64% of control sortilin-1 levels, AAV8-*Sort1* expression in *ob/ob* mice led to 35%, 34%, and 47% reductions at the 2.5-hour time point in secretion of TGs, apoB100, and apoB48, respectively, compared with *ob/ob* mice injected with control AAV8 (Figure 2, B–D). We also reconstituted sortilin-1 in DIO mice by AAV8-*Sort1* (Supplemental Figure 2A). As shown in Supplemental Figure 2, B and C, secretion of TGs, apoB100, and apoB48 was decreased in DIO mice after AAV-*Sort1* injection (Supplemental Figure 2, B and C).

mTORC1 plays a role in the regulation of sortilin-1. In view of the inverse relationship between mTOR activity and sortilin-1 expression noted above, we carried out further studies to test the hypoth-

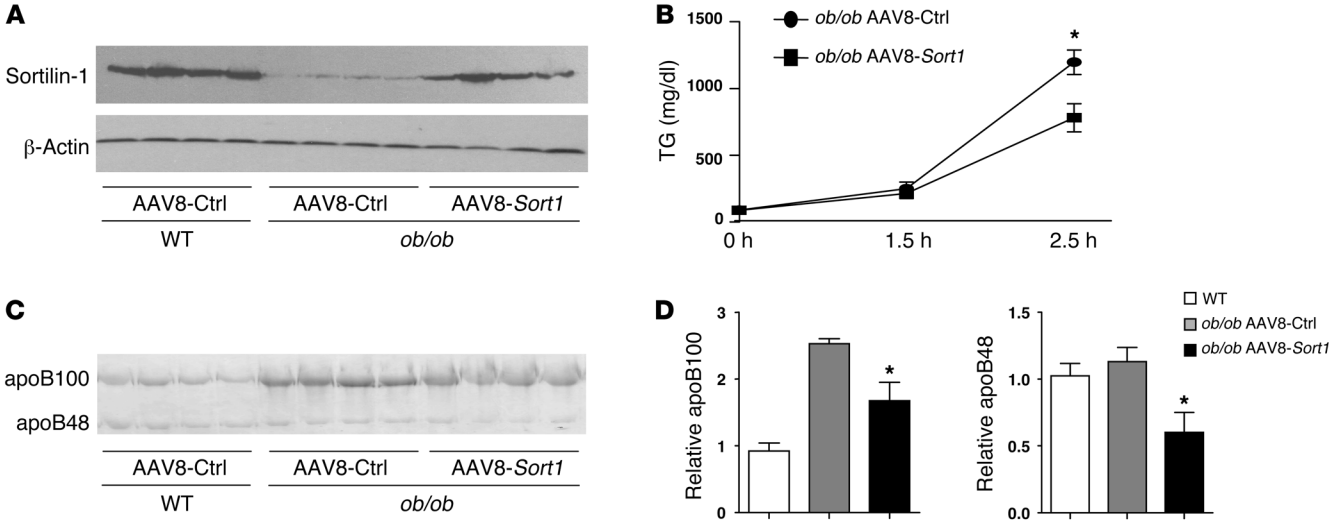

Figure 2

Restoration of sortilin-1 abolished apoB overproduction in *ob/ob* mice. (**A**) Hepatic protein expression of sortilin-1 in WT and *ob/ob* mice. Animals were fed WTD for 1 week before injection with control AAV8 or AAV8-*Sort1*, fed WTD for an additional 2 weeks, then sacrificed after a 6-hour fast. (**B**) TG production was determined at the indicated times after P407 injection. ANOVA revealed significant differences between treatment ($F_{2,14} = 8.753$; $P = 0.0034$) and time point (*$P < 0.05$ at 2.5 hours, Bonferroni post-test). (**C**) apoB levels in plasma collected at the 2.5-hour time point. (**D**) Quantification and ANOVA revealed significant differences between treatments for apoB100 ($F_{2,11} = 27.91$) and apoB48 ($F_{2,11} = 5.554$) from **C**. *$P < 0.05$, AAV8-*Sort1* vs. control AAV8, Bonferroni post-test.

esis that increased mTOR activity leads to repression of sortilin-1 expression. We used a genetic model of increased hepatic mTORC1 activity in which liver-specific KO of the upstream mTOR inhibitor *Tsc1* is obtained by injecting adeno-Cre into $Tsc1^{fl/fl}$ mice (referred to herein as $Li\text{-}Tsc1^{KO}$ mice). This resulted in a 15% increase in the liver weight/body weight ratio in $Li\text{-}Tsc1^{KO}$ mice versus $Tsc1^{fl/fl}$ controls (Figure 3E). Consistent with a previous report (27), *Atf3* was induced in $Li\text{-}Tsc1^{KO}$ mice (Figure 3, A and B). The protein and mRNA levels of sortilin-1 in $Li\text{-}Tsc1^{KO}$ mice were respectively decreased to 50% and 51% of control levels. In $Li\text{-}Tsc1^{KO}$ mice, *Srebp1c* and *Fas* were both decreased (Figure 3F), as recently reported by other groups (22, 34), possibly reflecting reduced AKT signaling. Consistent with the hypothesis that reduced sortilin-1 expression would lead to increased VLDL apoB secretion, apoB100 and apoB48 were increased 1.8- and 1.5-fold, respectively, in $Li\text{-}Tsc1^{KO}$ mice at the 2.5-hour time point (Figure 3C). Interestingly, however, TG secretion was not significantly changed (Figure 3D), probably reflecting reduced *Srebp1c* and lipogenic gene expression (Figure 3F). Thus, the liver appears to secrete increased numbers of apoB-containing lipoproteins that are relatively deficient in TG.

We next assessed whether reduction of hepatic mTORC1 activity might lead to increased *Sort1* expression. Treatment of *ob/ob* mice with rapamycin led to decreased hepatic mTORC1 activity, as shown by downregulation of ribosomal protein S6 kinase 1 phosphorylation (p-S6K; Supplemental Figure 3A) and increased levels of sortilin-1 protein and mRNA (Supplemental Figure 3, A and B). ER stress markers, such as p-eIF2α, Grp78, and Atf3, were repressed by rapamycin (Supplemental Figure 3A). We also used a genetic model of decreased hepatic mTORC1 activity, using primary hepatocytes from high-fat diet–fed $Raptor^{-/-}$ mice (Raptor is the regulatory component of mTORC1; ref. 35). $Raptor^{-/-}$ hepatocytes showed decreased mTORC1 activity, as shown by decreased expression of p-S6K, p-eIF2α, and Atf3 and increased expression of sortilin-1 (Supplemental Figure 3C).

Since hepatic insulin signaling is an important activator of mTOR, we also examined sortilin-1 expression in the $L1^{B6}Ldlr^{-/-}$ mouse strain, a transgenically rescued $Insr^{-/-}$ mouse strain on the $Ldlr^{-/-}$ background with genetically reduced (>90%) insulin receptors in the liver. The $L1^{B6}Ldlr^{-/-}$ mice and their control $Ldlr^{-/-}$ mice were fed WTD for 11 weeks. In contrast to *ob/ob* and DIO mice, the $L1^{B6}Ldlr^{-/-}$ mice showed elevated levels of hepatic *Sort1* mRNA (1.5-fold) and sortilin-1 protein (2.4-fold), in association with reduced mTOR activation and ER stress (Supplemental Figure 4, A and B). Our previous studies showed that apoB secretion was reduced in $L1^{B6}Ldlr^{-/-}$ compared with $Ldlr^{-/-}$ mice (30). To determine whether the increased expression of sortilin-1 in the livers of $L1^{B6}Ldlr^{-/-}$ mice was involved in this effect, we knocked down sortilin-1 expression in the liver using *Sort1*-siRNA (Supplemental Figure 4C), followed by injection of P407 to assess VLDL secretion. As shown in Supplemental Figure 4, D and E, the reduction of apoB and TG secretion in the $L1^{B6}Ldlr^{-/-}$ mice was largely reversed by sortilin-1 knockdown.

Role of ER stress in regulation of Sort1. Increased hepatic mTOR activity leads to induction of ER stress as a result of increased protein synthesis mediated by S6K (27, 36). To assess the role of ER stress in the suppression of *Sort1*, we treated WT mice with the ER stressor tunicamycin. This led to a marked repression of sortilin-1 expression, with a nadir 12 hours after tunicamycin treatment (Figure 4A). Tunicamycin caused induction of a variety of ER stress markers (data not shown), including the immediate early gene *Atf3*, which was induced prior to the maximal repression of *Sort1* (Figure 4B). This time course is consistent with a potential role for Atf3 in the transcriptional repression of *Sort1* (see below). In contrast, maximal CHOP induction occurred at a later time point, and tunicamycin was able to fully repress sortilin-1 in $Chop^{-/-}$ mice (Figure 4C).

PBA treatment alleviates ER stress, increases sortilin-1, and reduces VLDL secretion in ob/ob mice. To further explore a possible role of ER stress in the suppression of *Sort1* in vivo, we assessed whether suppression

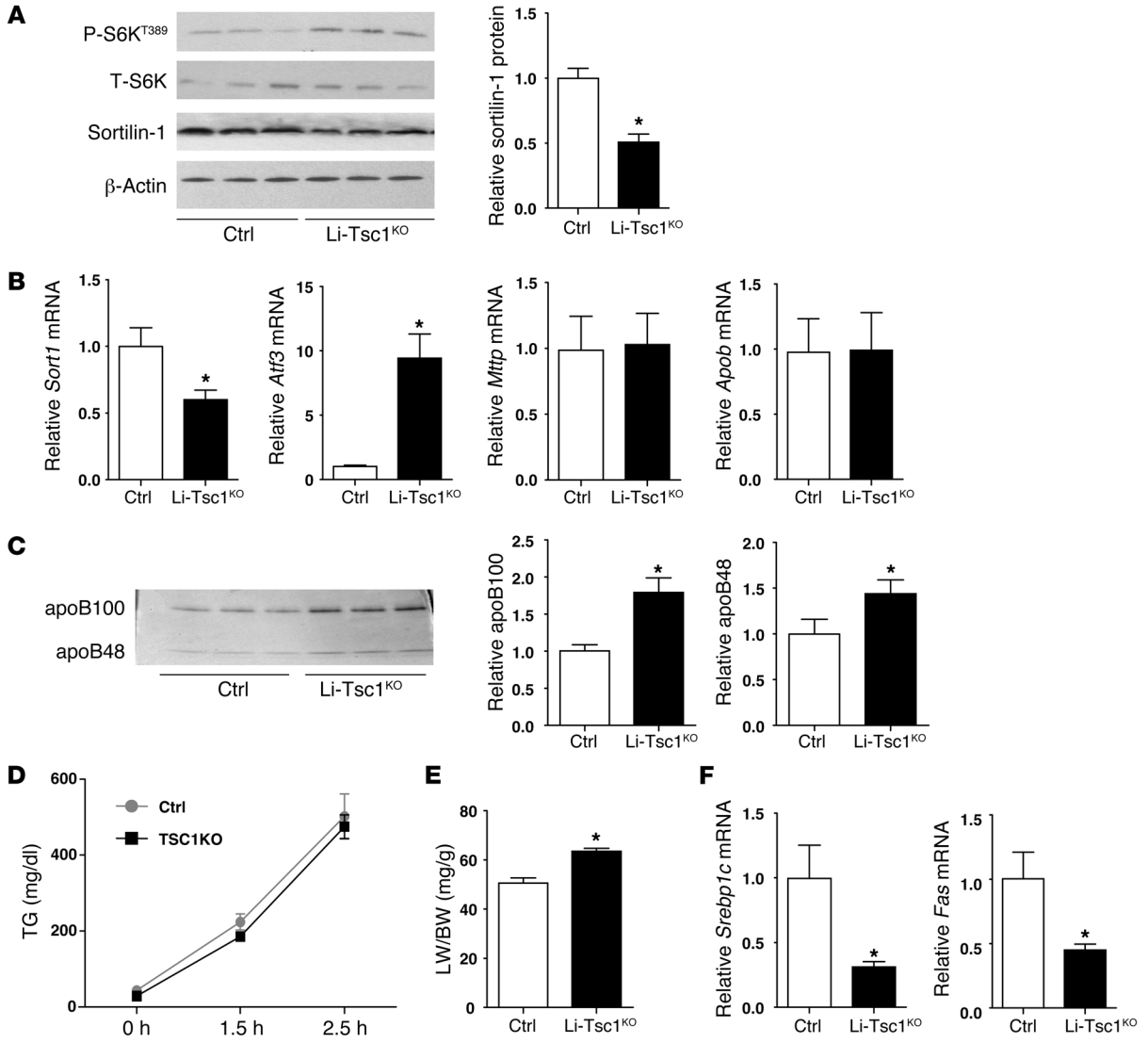

Figure 3

Downregulation of sortilin-1 in *Li-Tsc1^{KO}* mice. (**A**) Western blot analysis of hepatic S6K, sortilin-1, and β-actin protein levels in *Li-Tsc1^{KO}* and control mice sacrificed 7 days after injection (Cre and control adenovirus, respectively) via tail vein. (**B**) Hepatic *Sort1*, *Mttp*, *Apob*, and *Atf3* mRNA levels were measured by QPCR. (**C**) apoB levels in plasma collected at 2.5 hours; quantification is also shown. (**D**) TG production over time after P407 injection. ANOVA revealed significant differences only for time point ($F_{2, 12} = 134.3$; $P < 0.0001$), not for treatment. (**E**) Liver weight/body weight ratio (LW/BW). (**F**) Hepatic *Srebp1c* and *Fas* mRNA levels were measured by QPCR. *$P < 0.05$, unpaired *t* test.

of ER stress can block the regulation of sortilin-1. We administered the chemical chaperone 4-phenyl butyric acid (PBA), using a protocol that was previously shown to reduce hepatic ER stress in *ob/ob* mice (37, 38). Oral administration of PBA to *ob/ob* mice reduced plasma glucose levels and decreased hepatic levels of p-eIF2α and its downstream effector Atf3 (Figure 5, A and B), as reported previously (38). The relief of ER stress was associated with 1.9- and 2.3-fold increased mRNA and protein levels, respectively, of sortilin-1 (Figure 5, A and B). These data suggest that high mTORC1-induced ER stress causes repression of sortilin-1 in *ob/ob* mice. In agreement with a role of sortilin-1 in decreasing VLDL secretion (9), reduction of ER stress with PBA treatment in *ob/ob* mice significantly attenuated TG, apoB100, and apoB48 secretion (Figure 5, C and D). At 2.5 hours after P407 injection, the decrease in apoB100 and apoB48 levels (32% and 35%, respectively) was more marked than the decrease in TG (31%). There was no significant effect of PBA on *Mttp* or *Apob* mRNA levels or on insulin or total plasma cholesterol levels (Figure 5, B and E). Plasma glucose levels were reduced by PBA treatment (Figure 5E), consistent with previous reports (38). Knockdown of sortilin-1 by *Sort1*-siRNA reversed the reduction of apoB secretion by PBA (Supplemental Figure 5B) in the context of repressed ER stress, as shown by persistently decreased p-eIF2α and Atf3 (Supplemental Figure 5A). These data suggest that repression of *Sort1* expression downstream of increased hepatic ER stress in *ob/ob* mice leads to increased secretion of VLDL TG and apoB.

Mechanisms of Sort1 regulation by ER stress. As a complementary in vitro approach, we used the McArdle hepatoma cell line and showed that induction of ER stress resulted in repression of *Sort1*

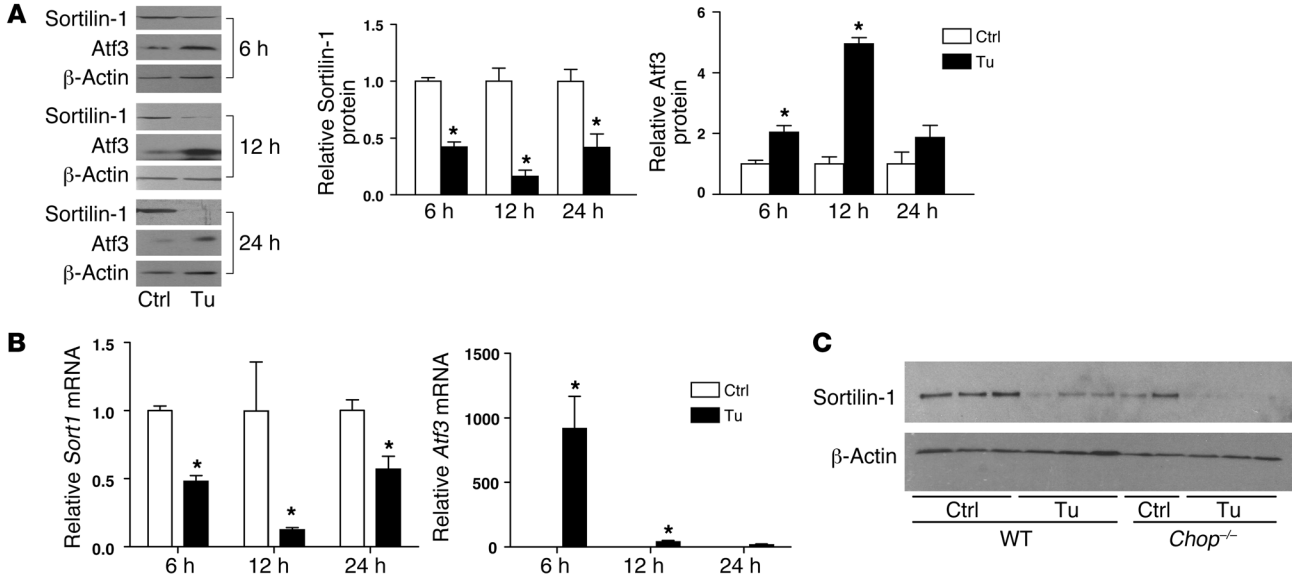

Figure 4

Tunicamycin decreased sortilin-1 expression in vivo. (**A**) Western blot analysis and quantification of hepatic sortilin-1 and Atf3 in WT mice injected with DMSO or tunicamycin (Tu; 1 mg/kg) for 6, 12, or 24 hours. (**B**) Hepatic *Sort1* and *Atf3* mRNA was determined by QPCR. (**C**) Western blot analysis of hepatic sortilin-1 in WT or *Chop*$^{-/-}$ mice injected with DMSO or 1 mg/kg tunicamycin for 24 hours. *$P < 0.05$ vs. control at the respective time point, unpaired *t* test.

expression. The mRNA levels of *Sort1* were decreased with tunicamycin treatment, with a nadir at 8 hours and partial recovery at 16 hours (Figure 6B); protein levels were similarly affected. We also used another ER stress inducer that works by a different mechanism: thapsigargin, an inhibitor of the ion transport activity of Ca^{2+}-ATPases of the sarcoplasmic and/or endoplasmic reticulum. This also resulted in a time-dependent reduction in sortilin-1 protein and mRNA levels and dramatic increases in ER stress markers, such as *Atf3* and *Grp78* (Figure 6, C and D).

Interestingly, actinomycin D treatment abolished the ability of tunicamycin to repress sortilin-1 expression in McArdle cells (Figure 6B), consistent with a requirement for synthesis of a transcriptional repressor in response to ER stress. In several settings in vivo and in cell culture, repression of *Sort1* was associated with induction of Atf3, a potential transcriptional repressor. We noted that the proximal promoter region of *SORT1* contains 2 potential ATF3 binding sites. Figure 7A shows these potential binding sites and their relationship to the putative causative SNP, which is associated with variation in hepatic *SORT1* expression in human populations and is located 3′ of the *SORT1* and *PSRC1* genes (9). Cotransfection of a 2.66-kb *SORT1* proximal promoter fragment linked to luciferase and an ATF3 expression vector resulted in repression of luciferase activity. Deletion of the more distal potential ATF3 binding site had no effect on luciferase activity repression by ATF3; however, deletion of the more proximal site led to loss of repressive activity (Figure 7B). Moreover, mutation of the proximal ATF3 binding site abolished the repression of luciferase activity by ATF3 cotransfection (Figure 7C). In contrast, overexpression of Atf3 via adenovirus vector (adeno-Atf3) in primary hepatocyte led to a reduction of sortilin-1 protein expression (Figure 7D). To examine whether *trans*-inactivation of the *SORT1* gene promoter by ATF3 binding is direct or indirect, we performed EMSA using oligonucleotide probes derived from the *SORT1* promoter. As shown in Figure 7E, thapsigargin treatment led to formation of specific DNA-protein complexes. Preincubation of nuclear extracts with 200× excess unlabeled oligonucleotide, mutant probe, or Atf3 antibody abolished the excess binding activity induced by thapsigargin (Figure 7E). To investigate whether Atf3 binds to the relevant proximal promoter site in vivo, we carried out ChIP assays in *Li-Tsc1*^{KO} and *ob/ob* mice, both of which showed markedly increased binding of Atf3 to the proximal promoter region corresponding to the human ATF3 binding site (Figure 7, F and G). There was also increased binding of Atf3 to its known binding site (39, 40) in the promoter of IL-6 in *ob/ob* and *Li-Tsc1*^{KO} mice.

Atf3 knockdown alleviates apoB and TG overproduction in ob/ob mice. To assess the in vivo role of Atf3 in the regulation of *Sort1* expression and VLDL secretion, we carried out *Atf3* siRNA knockdown. We knocked down Atf3 expression in the liver using *Atf3* versus control siRNA delivered in lipoid nanoparticles in *ob/ob* mice. As shown in Figure 8A, in vivo knockdown of Atf3 was effective (>80%) and led to an increase in sortilin-1 levels in *ob/ob* mice to the levels seen in WT mice. This was associated with a significant decrease in the secretion of TGs, apoB100, and apoB48 in *ob/ob* mice (Figure 8, B–D). In contrast, in WT mice, Atf3 levels were low, and the knockdown had no effect on *Sort1* expression or secretion of TGs or apoB (Figure 8, B–D).

Discussion

Our results demonstrate a major role of obesity and hepatic mTORC1 activity in the regulation of sortilin-1 expression and apoB secretion. Increased mTORC1 activity led to increased hepatic apoB secretion, at least in part via repression of hepatic *Sort1*, a gene recently implicated in the regulation of LDL cholesterol levels and coronary artery disease risk in human GWAS (9).

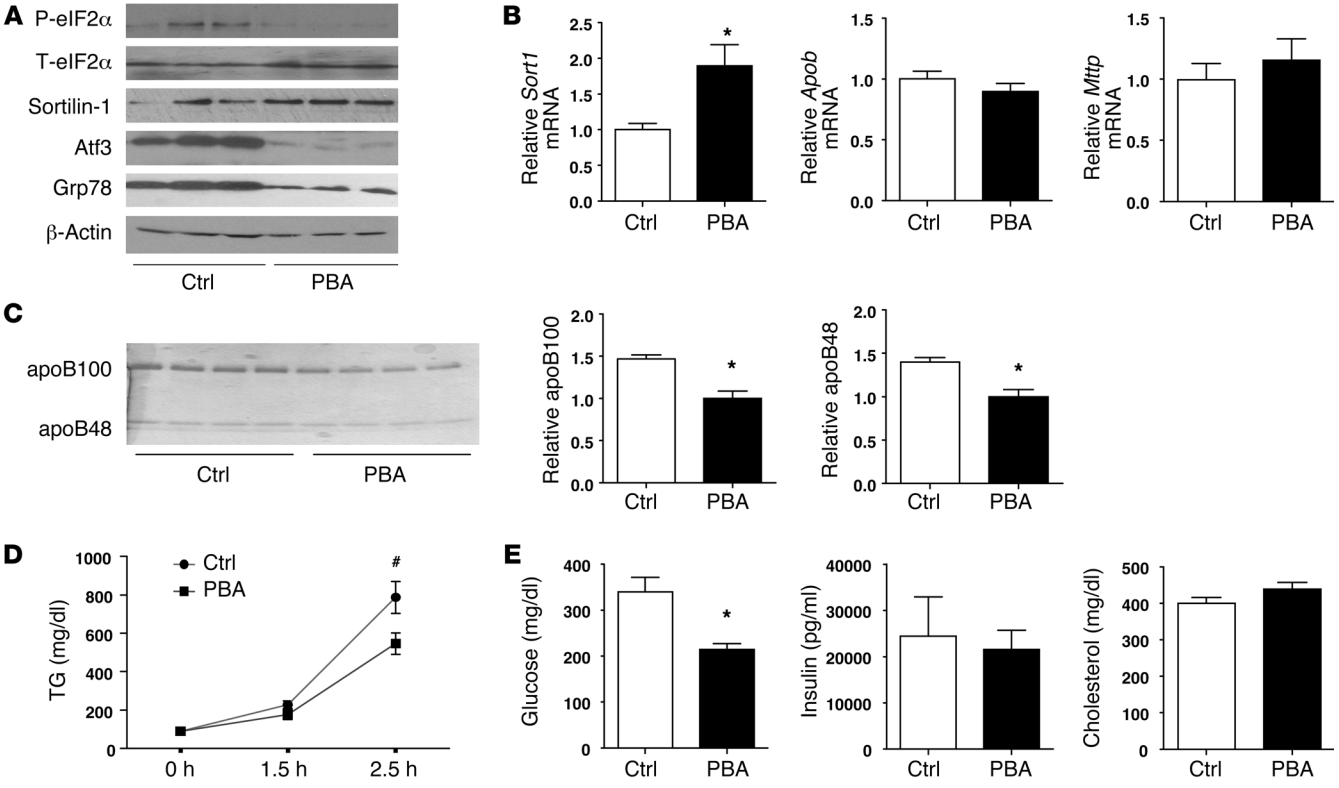

Figure 5

Expression of sortilin-1 was increased by suppression of ER stress. 8- to 10-week-old *ob/ob* mice were orally administered PBA (0.5 g/kg body weight, twice daily) or PBS control, fed WTD for 21 days, then fasted for 6 hours and subsequently killed. (**A**) Western blot analysis of hepatic p-eIF2α, total eIF2α, Atf3, Grp78, and sortilin-1 protein levels. (**B**) Hepatic *Sort1*, *Mttp*, and *Apob* mRNA levels were measured by QPCR. (**C**) apoB production was determined 2.5 hours after P407 injection; quantification is also shown. (**D**) TG secretion was determined. ANOVA revealed significant differences for treatment ($F_{2,46} = 4.385$; $P = 0.0181$) and time point ($^{\#}P < 0.05$ at 2.5 hours, Bonferroni post-test). (**E**) Basal levels of plasma glucose, insulin, and cholesterol were determined. $^{*}P < 0.05$, unpaired *t* test.

We showed that mTORC1 activation was associated with reduced *Sort1* expression in 2 different mouse models of obesity, *ob/ob* and DIO mice. A direct relationship between mTORC1 activation and *Sort1* repression was suggested by reversal of this effect with the mTORC1 inhibitor rapamycin and the demonstration that a well-characterized genetic model of increased mTORC1 activity, the *Li-Tsc1*^{KO} mouse, was also associated with suppression of *Sort1* (Figure 3A). Furthermore, hepatocytes from *Raptor*$^{-/-}$ mice with reduced mTORC1 activity showed increased *Sort1* expression. mTORC1 is known to activate ER stress, and we demonstrated that 2 different ER stressors, tunicamycin and thapsigargin, caused marked suppression of sortilin-1 protein and mRNA. We further showed reversal of sortilin-1 suppression in vivo by the chemical chaperone PBA, which ameliorated ER stress and its associated phenotypes in obese mice (Figure 5, A and C). PBA has previously been used to ameliorate ER stress in a variety of different settings (41–43), but may also have other activities (44). However, we showed that *Sort1* siRNA in conjunction with PBA reversed beneficial effects of apoB and TG, consistent with the proposed mechanism. Our findings with PBA were also consistent with several other approaches in which ER stressors caused repression of sortilin-1. On a mechanistic level, we demonstrated that the immediate early gene *ATF3*, which is rapidly induced by ER stress downstream of p-eIF2α, bound to a site in the proximal *SORT1* promoter and acted as a transcriptional repressor. Importantly, Atf3 knockdown by siRNA resulted in increased sortilin-1 and reduced TG and apoB secretion in *ob/ob* mice. Thus, chronic overnutrition and obesity may be linked to increased apoB production via a pathway involving mTORC1 activation and ER stress, with an important role for Atf3 in suppression of sortilin-1 and regulation of VLDL secretion.

Intriguingly, *Li-Tsc1*^{KO} mice demonstrated markedly increased secretion of apoB without a concomitant increase in TG secretion, likely reflecting the fact that *Srebp1c* and lipogenic gene expression are not increased in the livers of these mice (34, 35). Hepatic mTORC1 has been implicated in the regulation of *Srebp1c* and lipogenic gene expression (13). Recent studies have suggested that induction of *Srebp1c* and lipogenic gene expression in response to insulin signaling may require a dual signal involving both activation of mTORC1 and repression of Insig-2 (22). In addition, a novel pathway involving mTORC1 phosphorylation of cytoplasmic LIPIN-1, leading to its nuclear entry and stabilization of SREBPs, has recently been elucidated (21). Our findings demonstrate a clear dissociation between the regulation of hepatic apoB and TG secretion in vivo and highlight a specific role of sortilin-1 in the regulation of apoB secretion. However, in most of the other settings, variations in *Sort1* expression led to parallel effects on TG and apoB secretion. The level of TG secretion may be independently modulated by many factors, including

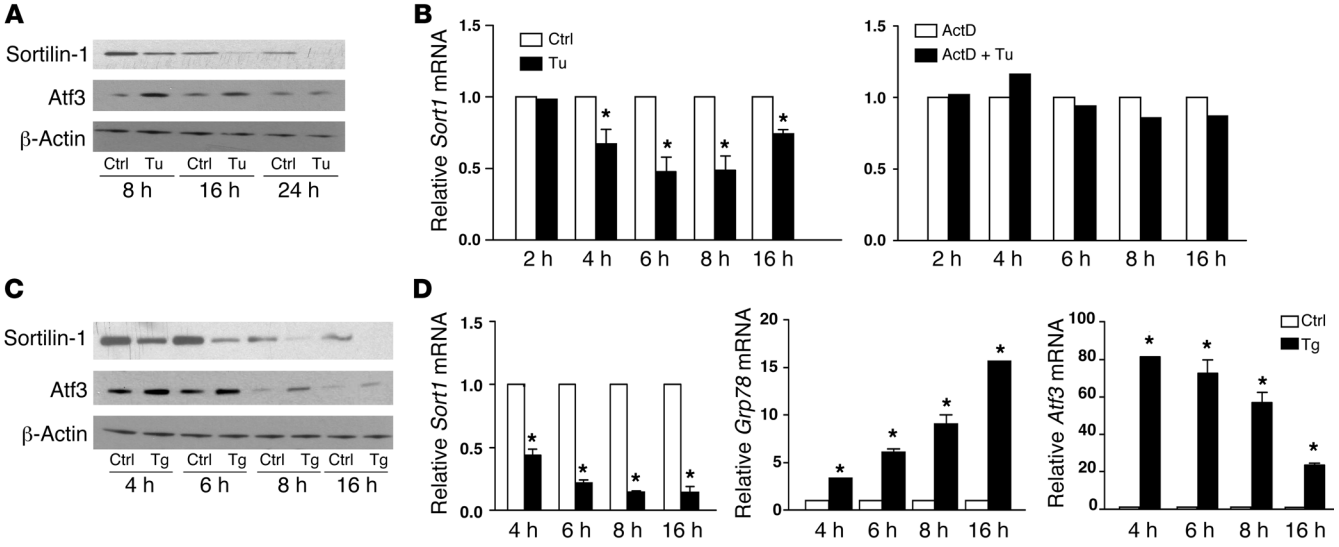

Figure 6

Regulation of sortilin-1 by ER stress. (**A**) Western blot analysis of sortilin-1 and Atf3 in cells of the McArdleH7777 line treated with DMSO or 5 μg/ml tunicamycin at the indicated time points. (**B**) *Sort1* mRNA was determined by QPCR. McArdle cells were treated with DMSO control or 5 μg/ml tunicamycin or were preincubated with 5 μg/ml actinomycin D (ActD) for 30 minutes with or without 5 μg/ml tunicamycin for the indicated times. (**C**) Western blot analysis of sortilin-1 and Atf3 protein levels in McArdle cells treated with 1 μM thapsigargin (Tg) for the indicated times. (**D**) *Grp78*, *Atf3*, and *Sort1* mRNA was measured by QPCR in McArdle cells treated with 1 μM thapsigargin for the indicated times. 3 separated experiments were performed. $^*P < 0.05$ vs. control for the respective time point, unpaired *t* test.

the levels of de novo lipogenesis, suggesting a complex pathway involving mTORC1 and Insig-2 (22), LIPIN-1 (21), and the flux of FFA from peripheral tissues (45).

The regulation of apoB secretion may occur on multiple levels in obesity. One factor may be moderately increased delivery of FFA to the liver, resulting in decreased degradation of apoB in the ER (46). In addition, administration of polyunsaturated fatty acids results in post-ER presecretory proteolysis (PERPP), involving PUFA-dependent ROS formation, aggregation of apoB, and degradation of aggregates via activation of autophagy (47). The relative importance of these various pathways in the regulation of hepatic apoB secretion will require further study. Our study, however, identifies chronic overnutrition involving several weeks of feeding a high-fat diet and mTOR activation in the regulation of sortilin-1 expression. While ER stress in obesity may involve a number of different mechanisms, the decrease in ER stress markers, along with reversal of changes in *Sort1* expression by rapamycin (Supplemental Figure 3A), indicates that increased mTORC1 activity is a major mechanism underlying these effects of obesity.

Recently, 2 reports have implicated *SORT1* as the causative gene underlying a human chromosome 1 LDL/coronary artery disease locus, but their authors came to opposite conclusions concerning the role of sortilin-1 in regulating apoB secretion. SNPs most strongly associated with LDL levels were localized to an intergenic region between *CELSR2* and *PSRC1* (11). The minor allele SNP with strongest association was shown to create a functional C/EBPα binding site (11), leading to an increase in the expression of *SORT1* in human hepatocytes. Studies in overexpressing and knockdown mice demonstrated that higher sortilin-1 levels were associated with reduced hepatic apoB secretion and lower LDL cholesterol levels. However, Kjolby et al. concluded the opposite: that decreased sortilin-1 expression is associated with lower levels of apoB exportation and LDL cholesterol, with sortilin-1 overexpression producing increased apoB exportation and LDL cholesterol levels (48). Possible reasons for the discrepancies have been reviewed, but the issue remains unresolved (49–52). However, it is notable that the major human SNP variant associated with increased plasma LDL cholesterol level is also associated with reduced hepatic *Sort1* expression. Moreover, in the present study, we found that in *ob/ob* mice, reduced levels of hepatic *Sort1* were associated with increased apoB secretion, with reversal by sortilin-1 overexpression, consistent with the findings of Musunuru et al. (11).

Our study demonstrated transcriptional repression of *Sort1* by Atf3, mediated via a binding site for ATF3 in the promoter region of *SORT1*. On a cellular level, Atf3 is an immediate early gene that is rapidly induced by ER stress, but as suggested here, it may also have a role in mediating effects of chronic ER stress. mTORC1 activation led to a general increase in protein and lipid synthesis, which may represent a cellular stress. apoB is a major secretory protein in the liver, and sortilin-1 repression by Atf3 leads to increased secretion of VLDL protein and lipid, perhaps helping to relieve the stress within the secretory pathway on a cellular/organelle level. This may also facilitate shunting of energy/calories away from the liver toward adipose tissue, and in that tissue, downregulation of *Sort1* in obesity (53) could potentially lead to increased LPL activity and uptake of VLDL TGs (16). Thus, the ATF3/*SORT1* mechanism could be viewed as an adaptation to relieve stress in hepatocytes by increasing VLDL secretion and promoting lipid storage in adipose. However, in the whole organism, the price to pay for this adaption may be an atherogenic lipoprotein profile.

Methods

Animals. ob/ob and C57BL/6 WT mice were purchased from The Jackson Laboratory. The length of WTD (40% kcal from fat; TD88137; Harlan Teklad) or high-fat diet (60% kcal from fat; D12492i; Research Diets Inc.) feeding is specified in the figure legends. Mice carrying a floxed allele of

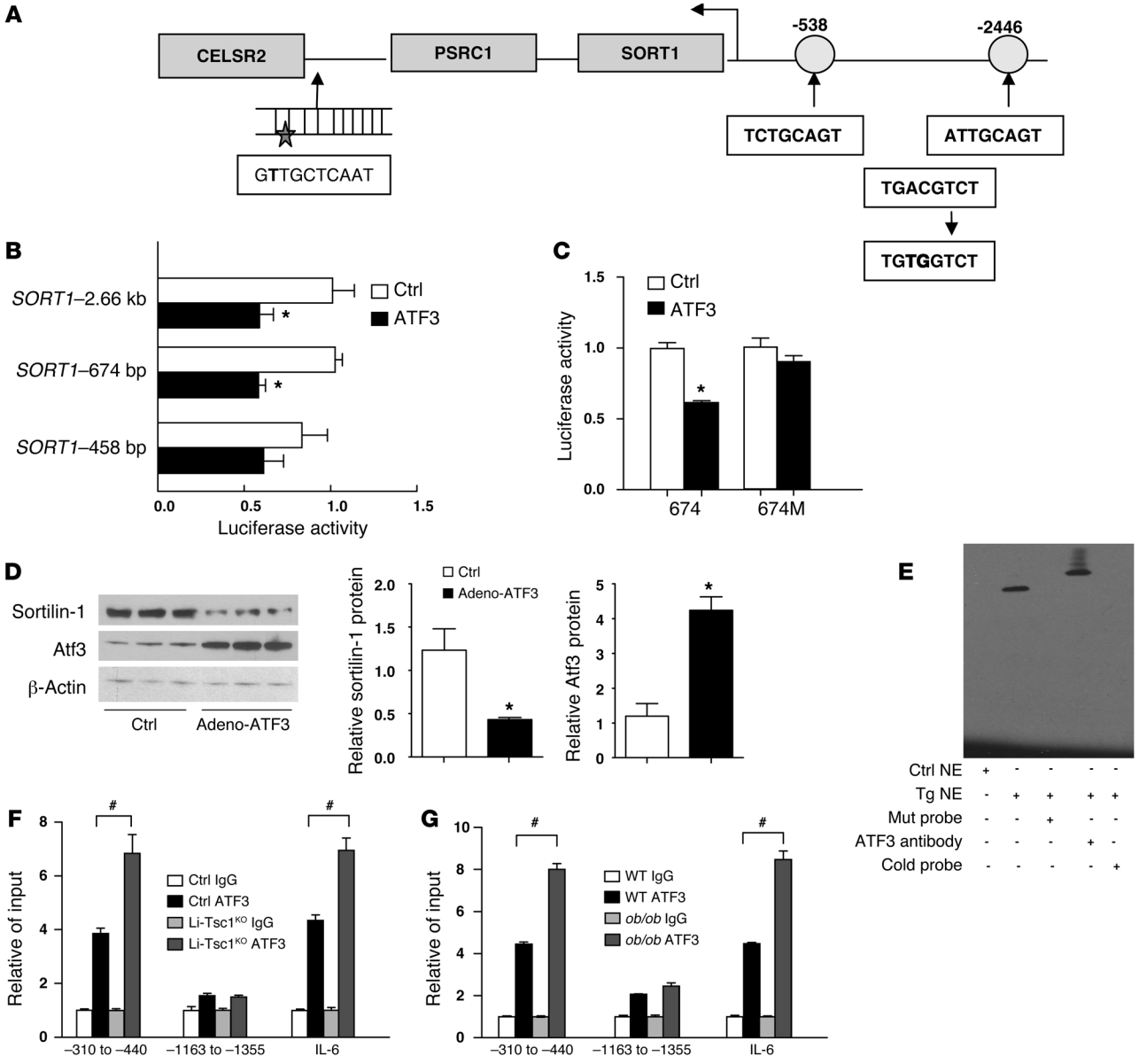

Figure 7

Mechanism of sortilin-1 regulation by ATF3. (**A**) 2 putative ATF3 binding sites were predicted in the *SORT1* promoter region. SNPs (asterisk) in CELSR2-PSRC1-SORT1 locis, which can regulate the expression of *SORT1*, identified a high association with CVD by GWAs studies. Two putative ATF3 binding sites were predicted in *SORT1* promoter region. (**B**) Human *SORT1* promoter fragments *SORT1*–2.66 kb, *SORT1*–674 bp, and *SORT1*–458 bp (see Methods) were inserted into the reporter system and cotransfected with or without ATF3 plasmid in the 293 cell line. (**C**) *SORT1*–674 bp was used as template to make a mutation construct (674M), and both were cotransfected with or without ATF3 in 293 cells. (**D**) Sortilin-1 expression was reduced by overexpressing adeno-Atf3 in mouse primary hepatocytes. Quantification is also shown. Empty adenoviral vector served as control. (**E**) EMSA was performed in the nuclear extract (NE) protein (5 μg) from 293 cells with biotin-labeled probes containing the ATF3 or mutant binding site in the *SORT1* promoter at –538 bp. Cells were treated directly with DMSO control or thapsigargin and preincubated with cold probe or ATF3 antibody. (**F** and **G**) ChIP analysis in *Li-Tsc1*^{KO} mice and *Li-Tsc1*$^{fl/fl}$ controls (**F**) and in *ob/ob* and control lean mice (**G**) using IgG or ATF3 antibody. The approximate –310 to –440 region in the mouse promoter is homologous to a region in the human promoter containing a proximal ATF3 binding site. ANOVA revealed significant differences for treatment with –310 to –440 primers (**F**, $F_{3,12} = 58.40$, $P < 0.0001$; **G**, $F_{3,15} = 523.1$, $P < 0.0001$) and IL-6 primers (**F**, $F_{3,12} = 127.0$, $P < 0.0001$; **G**, $F_{3,15} = 269.9$, $P < 0.0001$). *$P < 0.05$, unpaired *t* test. #$P < 0.05$ as shown by brackets, Bonferroni post-test.

Tsc1 (*Tsc1*$^{loxP/loxP}$) (54) were purchased from The Jackson Laboratory. 100 μl adenoviral-Cre or adenoviral-empty (5×10^{10} pfu•ml^{-1}) was administered via tail vein injection under isoflurane anesthesia to mice at 8 weeks of age. Mice were subjected to a 5-hour fast on the seventh day after injection and subsequently killed. *ob/ob* mice were fed WTD for 1 week before being injected with control AAV8 or AAV8-*Sort1* (1×10^{10} viral particles/mouse). After another 2 weeks of WTD feeding, mice were subjected to a 6-hour fast and subsequently killed. *ob/ob* mice (8–10 weeks old) fed WTD for 3

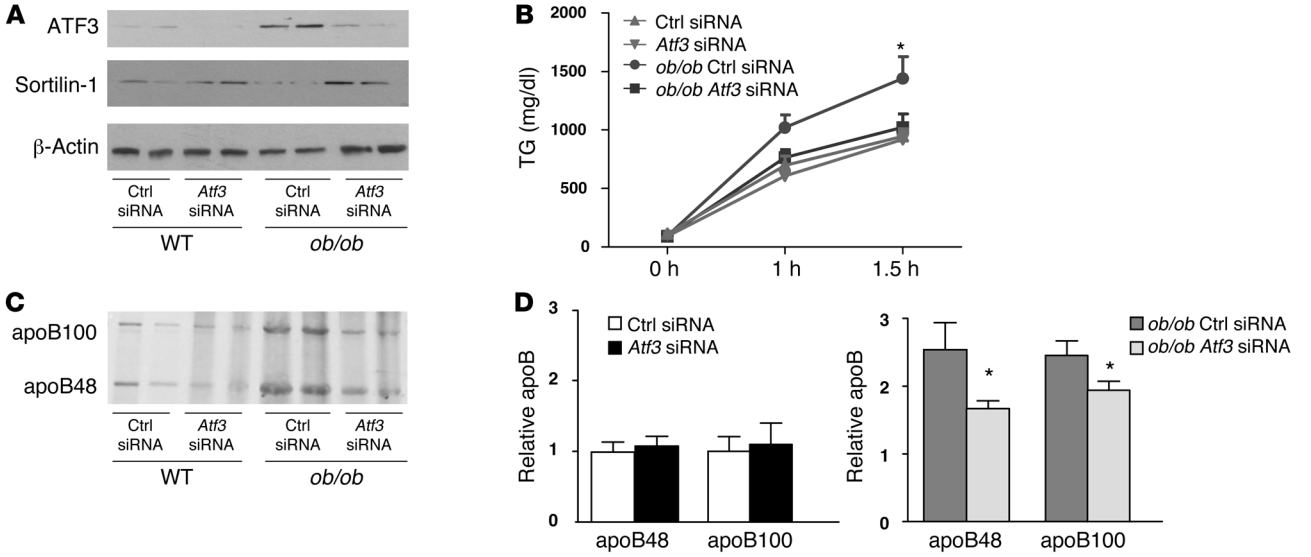

Figure 8

Atf3 deficiency rescued sortilin-1 expression and reduced apoB production in *ob/ob* mice. (**A**) WT and *ob/ob* mice were injected with control or *Atf3* siRNA, and expression of Atf3 and sortilin-1 was measured by Western blot. (**B**) Mice were fasted for 5 hours before TritonWR1339 and ^{35}S-methionine injection. TG secretion was measured at the indicated times after injection. ANOVA revealed significant differences for both treatment ($F_{6,34}$ = 3.103, P = 0.0156) and time point ($^{\#}P < 0.05$, control vs. *Atf3* siRNA in *ob/ob* animals at 1.5 hours, Bonferroni post-test). (**C**) Representative autoradiogram showing plasma apoB at the 2-hour time point. (**D**) Quantification of relative apoB levels of WT and *ob/ob* mice was performed by cutting out apoB100 and apoB48 bands for each sample and counting. $^{*}P < 0.05$, unpaired *t* test.

weeks were injected with rapamycin (20 mg/kg i.p.) and killed 24 hours later. *ob/ob* and lean mice (8–10 weeks old) were orally administered PBA (0.5 g/kg body weight twice per day), fed WTD for 21 days, then killed after a 6-hour fast. C57BL/6 WT and *Chop*$^{-/-}$ mice (55) were injected with tunicamycin (1 mg/kg body weight i.p.) for the indicated time courses. WT and *ob/ob* mice were injected with control or *Atf3* siRNA (1 mg/kg) for 3 days and killed after a 5-hour fast. Adeno-Atf3 was provided by M.R. Montminy (Salk Institute, La Jolla, California, USA). Mice had free access to food and water and were housed in a pathogen-free facility according to animal welfare guidelines. See Supplemental Methods for details.

Plasma glucose, insulin, cholesterol, and TG determination. Mice were fasted for 5–6 hours, and blood samples were collected by retroorbital venous plexus puncture. Plasma was separated by centrifugation and stored at –80°C until analyzed. TG, glucose, and insulin were measured with Infinity (Thermo Scientific), Trinder (Sigma-Aldrich), and an ELISA kit (Crystal Chem Inc.), respectively, according to the manufacturers' instructions.

apoB measurement. Plasma (100 μl) from mice fasted for 6 hours was used for apoB measurement. The major lipoproteins, VLDL, IDL, and LDL (combined density, 1.063 g/ml), were isolated by sequential density ultracentrifugation of plasma using a TLA-100 rotor (Beckman Coulter). apoB-containing lipoproteins were run on SDS-PAGE gels and visualized by 0.05% Coomassie blue staining (Sigma-Aldrich). The S^{35}-labeled apoB secretion assay method used in mice was as previously described (56).

TG production. The P407 method was used in mice to measure TG production rate in plasma (57). Mice fasted for 5–6 hours were injected with P407 (1,000 mg/kg i.p.; gift from BASF Customer Care). Blood samples were collected after injection at the times indicated in the figure legends. Plasma samples were used for TG determination.

Western blot analysis. Cell lysates were prepared and analysis was performed as described previously (30). Western blot analysis was carried out using the following primary antibodies: anti–p-mTOR (Cell Signaling Technology); anti–total mTOR (Cell Signaling Technology); anti–p-S6K (Cell signaling Technology), anti–sortilin-1 (Abcam), anti–p-eIF2α (Abcam), anti–total eIF2α (Cell signaling Technology), anti-ATF3 (Santa Cruz Biotechnology), and anti–β-actin (Sigma-Aldrich). Protein samples were separated by SDS-PAGE and transferred onto nitrocellulose membranes (Bio-Rad). Blots were probed separately with antibodies as indicated in the figures. After incubation with horseradish peroxidase–conjugated secondary antibodies, proteins were visualized with SuperSignal West Pico Chemiluminescent reagents (Pierce; Thermo Scientific) on X-ray films. When comparing phosphorylated and total protein, the same membrane incubated with phospho-protein antibody was detected by stripping-reprobing with total protein antibody. Band intensity was quantified using scanning densitometry of the autoradiogram with NIH ImageJ software (http://rsb.info.nih.gov/ij/).

Real-time quantitative PCR analysis. Liver tissues were homogenized, and total RNA was isolated using TRIzol (Invitrogen) according to the manufacturer's instructions. 2 μg total RNA was reverse transcribed at 50°C with First Strand cDNA Synthesis Kit (Fermentas). Real-time quantitative PCR (QPCR) was performed using the Mx4000 Multiplex Quantitative PCR System with 1 cycle at 95°C for 10 minutes followed by 40 cycles at 95°C for 30 seconds, 60°C for 30 seconds, and 72°C for 1 minute. The relative amounts of specific target amplicons for each primer set were estimated by a standard curve method using Mx4000 software (version 3.01; Stratagene) and were normalized to the copy number of housekeeping gene 36B4 or β-actin. See Supplemental Table 1 for primer sequences.

Luciferase expression constructs. The human *SORT1* promoter region was located according to the human genomic sequence of *Homo sapiens* chromosome 1 79912636–79915440. With the transcriptional start site of *SORT1* (promoter 2.0, for the recognition of PolII promoter sequences) designated as 0, the promoter region (–2,660 to –12) of the gene was amplified by PCR from the human bac clone (RP11-297O4) with the primer set 5′-CCCTTGCCGCACCTCTAGCG-3′ and 5′-TGCACTGTCCACAACATGGCT-3′. The amplified PCR products were subcloned into the

KpnI and XhoI sites of the pGL-4.10 basic vector (Invitrogen). The generated plasmid with the *SORT1* promoter linked to luciferase (Luc) reporter was designated *SORT1*–2.66 kb. For a series of *SORT1* promoter deletion constructs (i.e., *SORT1*–674 bp and *SORT1*–458 bp), the corresponding fragments were amplified by PCR with *SORT1*–2.66 kb used as the template and the following primer sets: *SORT1*–674 bp, 5′-GGCC′GGTACC′GCGGTAAAGGGAACAGCGTAGG-3′; *SORT1*–458 bp, 5′-GGCC′CTCGAG′CCCTTGCCGCACCTCTAGCG-3′. *SORT1*–674 bp was used as template to make a mutation construct (Quikchange site-directed mutagenesis kit; Agilent). For transient transfection, plasmid DNA was transfected into 293 cells by use of the Lipofectamine 2000 method (Invitrogen). RL-TK was cotransfected as a transfection control. Plasmid ATF3 was provided by L. Qi (Cornell University, Ithaca, New York, USA). After various treatments, cells were lysed and measured by the Dual Luciferase Reporter (DLR) Assay System (Promage).

EMSA. Nuclear extracts were prepared according to the manufacturer's protocols (NE-PER nuclear and cytoplasmitic extraction reagents; Thermo Scientific). The sequences of the biotin-labeled probe and cold probe were 5′-AGGCTTCGAGAGTGACGTCTCAATTCC-3′ and 5′-GGAATTGAGACGTCACTCTCGAAGCCT-3′. The biotin-labeled mutant probe sequences were 5′-AGGCTTCGAGAGTG**TG**GTCTCAATTCC-3′ and 5′-GGAATTGAGACCACACTCTCGAAGCCT-3′ (mutation shown in bold). For competition assay, nuclear extract protein from thapsigargin-treated 293 cells was preincubated with the unlabeled oligonucleotide (200× excess) or ATF3 antibody (Santa Cruz Biotechnology) for 10 minutes. DNA-protein complexes were resolved by 5% nondenaturing polyacrylamide gel and developed using the protocol of LightShift Chemiluminescent EMSA kit (Thermo Scientific).

ChIP assays. For chromatin lysates from mouse livers, liver tissue were crosslinked in 1% formaldehyde for 15 minutes, and liver nuclei were isolated (NE-PER; Pierce), followed by sonication. After being precleared with protein G agarose beads, chromatin lysates were immunoprecipitated using antibodies against ATF3 (Santa Cruz Biotechnology Inc.) or control rabbit IgG in the presence of BSA and salmon sperm DNA. Beads were extensively washed before reverse cross-linking. Sample DNA was isolated from the immunoprecipitates, then amplified by QPCR using primers flanking the enhancer or the proximal promoter regions (Supplemental Table 1). Detection of Atf3 binding to the IL-6 promoter (–230 to +31) in vivo (40) by ATF3 antibody was used as a positive control.

Statistics. Results are expressed as mean ± SEM; *n* is indicated in the figures and/or legends. Results were analyzed by 2-tailed Student's *t* test or 1- or 2-way ANOVA where appropriate, using GraphPad Prism software. A Bonferroni post-hoc test was used to test for significant differences revealed by ANOVA. A *P* value less than 0.05 was considered statistically significant.

Study approval. All animal experiments were reviewed and approved by the Columbia University Institutional Animal Care and Use Committee and were conducted according to that committee's guidelines.

Acknowledgments

Work in A. Tall's lab is supported by NIH grant HL087123. Akin Akinc and his team provided formulation support; Muthiah Manoharan, Martin Maier, Satya Kuchimanchi, and Klaus Charisse and their teams provided chemistry support. We thank Carrie Welch for statistical consulting.

Received for publication October 3, 2011, and accepted in revised form February 15, 2012.

Address correspondence to: Ding Ai, Columbia University Medical Center, P&S8-401, 630 West 168th Street, New York, New York 10032, USA. Phone: 212.305.5789; Fax: 212.305.5052; E-mail: da2424@columbia.edu.

1. Adiels M, et al. Overproduction of VLDL1 driven by hyperglycemia is a dominant feature of diabetic dyslipidemia. *Arterioscler Thromb Vasc Biol*. 2005;25(8):1697–1703.
2. Myerson M, et al. Treatment with high-dose simvastatin reduces secretion of apolipoprotein B-lipoproteins in patients with diabetic dyslipidemia. *J Lipid Res*. 2005;46(12):2735–2744.
3. Nigro J, Osman N, Dart AM, Little PJ. Insulin resistance and atherosclerosis. *Endocr Rev*. 2006;27(3):242–259.
4. Riches FM, Watts GF, Naoumova RP, Kelly JM, Croft KD, Thompson GR. Hepatic secretion of very-low-density lipoprotein apolipoprotein B-100 studied with a stable isotope technique in men with visceral obesity. *Int J Obes Relat Metab Disord*. 1998;22(5):414–423.
5. Young SG. Recent progress in understanding apolipoprotein B. *Circulation*. 1990;82(5):1574–1594.
6. Fisher EA, Ginsberg HN. Complexity in the secretory pathway: the assembly and secretion of apolipoprotein B-containing lipoproteins. *J Biol Chem*. 2002;277(20):17377–17380.
7. Yao Z, Tran K, McLeod RS. Intracellular degradation of newly synthesized apolipoprotein B. *J Lipid Res*. 1997;38(10):1937–1953.
8. Willer CJ, et al. Newly identified loci that influence lipid concentrations and risk of coronary artery disease. *Nat Genet*. 2008;40(2):161–169.
9. Musunuru K, et al. From noncoding variant to phenotype via SORT1 at the 1p13 cholesterol locus. *Nature*. 2010;466(7307):714–719.
10. Kathiresan S, et al. Six new loci associated with blood low-density lipoprotein cholesterol, high-density lipoprotein cholesterol or triglycerides in humans. *Nat Genet*. 2008;40(2):189–197.
11. Musunuru K, et al. From noncoding variant to phenotype via SORT1 at the 1p13 cholesterol locus. *Nature*. 2010;466(7307):714–719.
12. Kathiresan S, et al. Genome-wide association of early-onset myocardial infarction with single nucleotide polymorphisms and copy number variants. *Nat Genet*. 2009;41(3):334–341.
13. Canuel M, Korkidakis A, Konnyu K, Morales CR. Sortilin mediates the lysosomal targeting of cathepsins D and H. *Biochem Biophys Res Commun*. 2008;373(2):292–297.
14. Lemansky P, Fester I, Smolenova E, Uhlander C, Hasilik A. The cation-independent mannose 6-phosphate receptor is involved in lysosomal delivery of serglycin. *J Leukoc Biol*. 2007;81(4):1149–1158.
15. McCormick PJ, Dumaresq-Doiron K, Pluviose AS, Pichette V, Tosato G, Lefrancois S. Palmitoylation controls recycling in lysosomal sorting and trafficking. *Traffic*. 2008;9(11):1984–1997.
16. Nielsen MS, Jacobsen C, Olivecrona G, Gliemann J, Petersen CM. Sortilin/neurotensin receptor-3 binds and mediates degradation of lipoprotein lipase. *J Biol Chem*. 1999;274(13):8832–8836.
17. Nilsson SK, Christensen S, Raarup MK, Ryan RO, Nielsen MS, Olivecrona G. Endocytosis of apolipoprotein A-V by members of the low density lipoprotein receptor and the VPS10p domain receptor families. *J Biol Chem*. 2008;283(38):25920–25927.
18. Shi J, Kandror KV. Sortilin is essential and sufficient for the formation of Glut4 storage vesicles in 3T3-L1 adipocytes. *Dev Cell*. 2005;9(1):99–108.
19. Kapahi P, et al. With TOR, less is more: a key role for the conserved nutrient-sensing TOR pathway in aging. *Cell Metab*. 2010;11(6):453–465.
20. Li S, Brown MS, Goldstein JL. Bifurcation of insulin signaling pathway in rat liver: mTORC1 required for stimulation of lipogenesis, but not inhibition of gluconeogenesis. *Proc Natl Acad Sci U S A*. 2010;107(8):3441–3446.
21. Peterson TR, et al. mTOR Complex 1 Regulates Lipin 1 Localization to Control the SREBP Pathway. *Cell*. 2011;146(3):408–420.
22. Yecies JL, et al. Akt Stimulates Hepatic SREBP1c and Lipogenesis through Parallel mTORC1-Dependent and Independent Pathways. *Cell Metab*. 2011;14(1):21–32.
23. Garami A, et al. Insulin activation of Rheb, a mediator of mTOR/S6K/4E-BP signaling, is inhibited by TSC1 and 2. *Mol Cell*. 2003;11(6):1457–1466.
24. Saucedo LJ, Gao X, Chiarelli DA, Li L, Pan D, Edgar BA. Rheb promotes cell growth as a component of the insulin/TOR signalling network. *Nat Cell Biol*. 2003;5(6):566–571.
25. Wellen KE, Hotamisligil GS. Inflammation, stress, and diabetes. *J Clin Invest*. 2005;115(5):1111–1119.
26. Ozcan U, et al. Endoplasmic reticulum stress links obesity, insulin action, and type 2 diabetes. *Science*. 2004;306(5695):457–461.
27. Ozcan U, et al. Loss of the tuberous sclerosis complex tumor suppressors triggers the unfolded protein response to regulate insulin signaling and apoptosis. *Mol Cell*. 2008;29(5):541–551.
28. Tremblay F, et al. Identification of IRS-1 Ser-1101 as a target of S6K1 in nutrient- and obesity-induced insulin resistance. *Proc Natl Acad Sci U S A*. 2007;104(35):14056–14061.
29. Bartels ED, Lauritsen M, Nielsen LB. Hepatic expression of microsomal triglyceride transfer protein and in vivo secretion of triglyceride-rich lipoproteins are increased in obese diabetic mice. *Diabetes*. 2002;51(4):1233–1239.
30. Han S, et al. Hepatic insulin signaling regulates VLDL secretion and atherogenesis in mice. *J Clin Invest*. 2009;119(4):1029–1041.
31. Jiang HY, et al. Activating transcription factor 3 is

integral to the eukaryotic initiation factor 2 kinase stress response. *Mol Cell Biol*. 2004;24(3):1365–1377.
32. Cunha DA, et al. Initiation and execution of lipotoxic ER stress in pancreatic beta-cells. *J Cell Sci*. 2008;121(pt 14):2308–2318.
33. Merat S, Casanada F, Sutphin M, Palinski W, Reaven PD. Western-type diets induce insulin resistance and hyperinsulinemia in LDL receptor-deficient mice but do not increase aortic atherosclerosis compared with normoinsulinemic mice in which similar plasma cholesterol levels are achieved by a fructose-rich diet. *Arterioscler Thromb Vasc Biol*. 1999;19(5):1223–1230.
34. Kenerson HL, Yeh MM, Yeung RS. Tuberous sclerosis complex-1 deficiency attenuates diet-induced hepatic lipid accumulation. *PLoS One*. 2011;6(3):e18075.
35. Sengupta S, Peterson TR, Laplante M, Oh S, Sabatini DM. mTORC1 controls fasting-induced ketogenesis and its modulation by ageing. *Nature*. 2011;468(7327):1100–1104.
36. Um SH, D'Alessio D, Thomas G. Nutrient overload, insulin resistance, and ribosomal protein S6 kinase 1, S6K1. *Cell Metab*. 2006;3(6):393–402.
37. Welch WJ, Brown CR. Influence of molecular and chemical chaperones on protein folding. *Cell Stress Chaperones*. 1996;1(2):109–115.
38. Ozcan U, et al. Chemical chaperones reduce ER stress and restore glucose homeostasis in a mouse model of type 2 diabetes. *Science*. 2006;313(5790):1137–1140.
39. Inouye S, et al. Heat shock transcription factor 1 opens chromatin structure of interleukin-6 promoter to facilitate binding of an activator or a repressor. *J Biol Chem*. 2007;282(45):33210–33217.
40. Takii R, et al. Heat shock transcription factor 1 inhibits expression of IL-6 through activating transcription factor 3. *J Immunol*. 2010;184(2):1041–1048.
41. Zode GS, et al. Reduction of ER stress via a chemical chaperone prevents disease phenotypes in a mouse model of primary open angle glaucoma. *J Clin Invest*. 2011;121(9):3542–3553.
42. Inoki K, et al. mTORC1 activation in podocytes is a critical step in the development of diabetic nephropathy in mice. *J Clin Invest*. 2011;121(6):2181–2196.
43. Basseri S, Lhotak S, Sharma AM, Austin RC. The chemical chaperone 4-phenylbutyrate inhibits adipogenesis by modulating the unfolded protein response. *J Lipid Res*. 2009;50(12):2486–2501.
44. Daosukho C, et al. Phenylbutyrate, a histone deacetylase inhibitor, protects against Adriamycin-induced cardiac injury. *Free Radic Biol Med*. 2007;42(12):1818–1825.
45. Boden G. Role of fatty acids in the pathogenesis of insulin resistance and NIDDM. *Diabetes*. 1997;46(1):3–10.
46. Ginsberg HN, Fisher EA. The ever–expanding role of degradation in the regulation of apolipoprotein B metabolism. *J Lipid Res*. 2009;50 suppl:S162–S166.
47. Pan M, et al. Presecretory oxidation, aggregation, and autophagic destruction of apoprotein-B: a pathway for late-stage quality control. *Proc Natl Acad Sci U S A*. 2008;105(15):5862–5867.
48. Kjolby M, et al. Sort1, encoded by the cardiovascular risk locus 1p13.3, is a regulator of hepatic lipoprotein export. *Cell Metab*. 2010;12(3):213–223.
49. Tall AR, Ai D. Sorting out sortilin. *Circ Res*. 2011;108(2):158–160.
50. Marian AJ. Genome-wide association studies complemented with mechanistic biological studies identify sortilin 1 as a novel regulator of cholesterol trafficking. *Curr Atheroscler Rep*. 2011;13(3):190–192.
51. Dube JB, Johansen CT, Hegele RA. Sortilin: an unusual suspect in cholesterol metabolism: from GWAS identification to in vivo biochemical analyses, sortilin has been identified as a novel mediator of human lipoprotein metabolism. *Bioessays*. 2011;33(6):430–437.
52. Calkin AC, Tontonoz P. Genome-wide association studies identify new targets in cardiovascular disease. *Sci Transl Med*. 2010;2(48):48ps46.
53. Kaddai V, et al. Involvement of TNF-alpha in abnormal adipocyte and muscle sortilin expression in obese mice and humans. *Diabetologia*. 2009;52(5):932–940.
54. Uhlmann EJ, et al. Astrocyte-specific TSC1 conditional knockout mice exhibit abnormal neuronal organization and seizures. *Ann Neurol*. 2002;52(3):285–296.
55. Zinszner H, et al. CHOP is implicated in programmed cell death in response to impaired function of the endoplasmic reticulum. *Genes Dev*. 1998;12(7):982–995.
56. Ota T, Gayet C, Ginsberg HN. Inhibition of apolipoprotein B100 secretion by lipid-induced hepatic endoplasmic reticulum stress in rodents. *J Clin Invest*. 2008;118(1):316–332.
57. Millar JS, Cromley DA, McCoy MG, Rader DJ, Billheimer JT. Determining hepatic triglyceride production in mice: comparison of poloxamer 407 with Triton WR-1339. *J Lipid Res*. 2005; 46(9):2023–2028.